TSUNAMI HAZARD ASSESSMENT ALONG THE COAST OF LINGAYEN GULF, PANGASINAN, PHILIPPINES

Julius Galdiano* **Supervisor: Yushiro FUJII****
MEE12621

ABSTRACT

We performed tsunami simulations for the Lingayen Gulf using the earthquake parameters of the two earthquake scenarios along the Manila Trench. The Case 1 earthquake scenario (M7.6) with a slip amount of 1.2 m produced smaller maximum wave height of 0.3 m and it arrived in about 1 hour in the inner bay of the Lingayen Gulf. The simulation results showed that Case 2 earthquake scenario (M8.4) with a slip amount of 3.7 m produced the maximum wave height of 1.6 m that arrived in about 1 hour in the inner bay of the Lingayen Gulf. The inundation computations showed that Case 1 produced a maximum height of 0.7 m and inundated approximately 0.13 km^2 in a target area in Dagupan City while Case 2 produced a maximum height of 3 m and inundated approximately 0.70 km^2 in the same area. The existing tsunami sensor (ASTI tide gauge station) is effective in the inner bay as it alarms the community of an impending tsunami in 30 min and 35 min in Cases 1 and 2, respectively, while it is ineffective in Bolinao coast because there will be a sudden tsunami arrival. Combining ASTI and JICA (proposed tsunami sensor project) tide gauge stations would advance to a better and robust tsunami early warning system in the Lingayen Gulf.

Keywords: Scenario earthquakes, Manila Trench, Tsunami numerical simulation, Tsunami sensor

1. INTRODUCTION

The geographical location of the Philippines makes the whole archipelago seismically active and prone to earthquakes, and offshore earthquakes can cause tsunamis.

PHIVOLCS has taken research on tsunami hazard and risk assessment in various areas to mitigate the future tsunami effects. One of the projects that were accomplished is the development of the first ever Community Tsunami Detection and Warning System in the Philippines in Pangasinan (Figure 1). The detection system is composed of three types of sensors: wet, dry and ultrasonic sea level monitoring (PHIVOLCS Website). As soon as the system detects a tsunami, the alarm systems installed in various areas will be triggered and alerts the communities to an impending tsunami threat.

Lingayen Gulf (see Figure 1) was selected as the study area because of its vulnerability to tsunami hazards and is close to Manila Trench which was the source of tsunamis that affected the nearby coastal areas in the past.

The purpose of the study is to assess the tsunami

Figure 1. Location of the study area with the existing tsunami early warning system (yellow star: tsunami sensor, red stars: sirens

*Philippine Institute of Volcanology and Seismology (PHIVOLCS)- Department of Science and Technology (DOST), Philippines
**International Institute of Earthquake Engineering (IISEE), Building Research Institute (BRI), Japan

hazard along the coasts of the Pangasinan Province where earthquakes and tsunamis have occurred as early as about 6,000 years ago (Ramos and Tsutsumi, 2010). We also discuss the effectiveness of the existing near real-time tsunami detector and warning systems in the Lingayen Gulf.

2. THEORETICAL CONCEPTS

2.1. Governing Equations in Cartesian and Spherical Coordinate Systems

In Cartesian coordinates, the shallow water wave equations (Imamura et al., 2006) can be written as

$$\frac{\partial \eta}{\partial t} + \frac{\partial M}{\partial x} + \frac{\partial N}{\partial y} = 0 \tag{1}$$

$$\frac{\partial M}{\partial t} + \frac{\partial}{\partial y}\left(\frac{M^2}{D}\right) + \frac{\partial}{\partial y}\left(\frac{MN}{D}\right) + gD\frac{\partial \eta}{\partial x} + \frac{gn^2}{D^{7/3}}M\sqrt{M^2+N^2} = 0 \tag{2}$$

$$\frac{\partial N}{\partial t} + \frac{\partial}{\partial x}\left(\frac{M^2}{D}\right) + \frac{\partial}{\partial y}\left(\frac{N^2}{D}\right) + gD\frac{\partial \eta}{\partial y} + \frac{gn^2}{D^{7/3}}N\sqrt{M^2+N^2} = 0 \tag{3}$$

where, D is the total water depth, η is the wave amplitude, t is the time, n is the roughness coefficient, M and N are the discharge fluxes in x and y directions, g is the gravitational acceleration.

Employing the spherical coordinate system in the numerical simulation is imperative to accommodate the spheroidal shape of the earth in the computation (Yanagisawa, 2013). The continuity and momentum equations are expressed as

$$\frac{\partial \eta}{\partial t} + \frac{1}{Rcos\theta}\left[\frac{\partial M}{\partial \lambda} + \frac{\partial}{\partial \theta}N(cos\theta)\right] = 0 \tag{4}$$

$$\frac{\partial M}{\partial t} + \frac{gD}{Rcos\theta}\frac{\partial \eta}{\partial \lambda} + \frac{1}{Rcos\theta}\frac{\partial}{\partial \lambda}\left(\frac{M^2}{D}\right) + \frac{1}{Rcos\theta}\frac{\partial}{\partial \theta}\left(cos\theta\frac{\partial MN}{D}\right) + \frac{gn^2}{D^{\frac{7}{3}}}M\sqrt{M^2+N^2} = 0 \tag{5}$$

$$\frac{\partial N}{\partial t} + \frac{gD}{Rcos\theta}\frac{\partial}{\partial \theta}(cos\theta\eta) + \frac{1}{Rcos\theta}\frac{\partial}{\partial \lambda}\left(cos\theta\frac{N^2}{D}\right) + \frac{1}{Rcos\theta}\frac{\partial}{\partial \lambda}\left(\frac{MN}{D}\right) + \frac{gn^2}{D^{\frac{7}{3}}}N\sqrt{M^2+N^2} = 0 \tag{6}$$

where, M is the discharge flux in the λ (along a parallel of latitude) direction, N is the discharge flux in the θ (along a parallel of longitude) direction, and R is the radius of the earth at 6378.137 km.

2.2. Ocean Floor Deformation

Ocean floor deformation is the initial condition to generate a tsunami. Vertical deformation of the ocean floor is assumed to be the same as the water surface displacement. To calculate this deformation, the elastic fault model by Okada (1985) using the fault plane model is used.

In this study, the effect of the horizontal displacement (Tanioka and Satake, 1996) is also considered. The vertical displacement of water due to the horizontal movement of the slope, $u_{h,}$ is calculated as

$$u_h = u_x\frac{\partial H}{\partial x} + u_y\frac{\partial H}{\partial y} \tag{7}$$

where, H is the water depth and u_x and u_y are the horizontal seafloor displacements due to a faulting.

3. DATA AND METHODOLOGY

3.1. Bathymetry and Topography Data

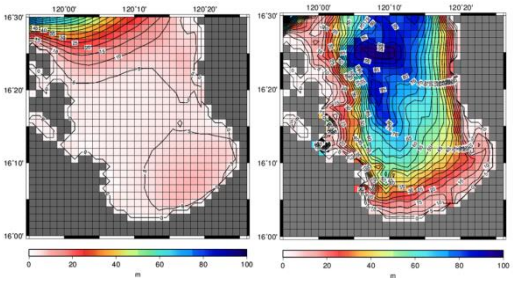

Figure 2. Comparison of the bathymetry data of G1m (right) and G30cD (left).

In this study, we used the bathymetry data from the General Bathymetry Chart of the Ocean (GEBCO) with resolutions of 1 arc-min (hereafter referred to as G1m) and 30 arc-sec (hereafter referred to as G30c) that were downloaded from the GEBCO website. To generate a finer resolution, the Philippine topography map with bathymetry data produced by the National Mapping and Resource Information Authority (NAMRIA, 1987) were digitized and merged to the GEBCO 30 arc-sec bathymetry data (hereafter G30cD) (Figure 2). The Shuttle Radar Topography Mission version 2 (SRTM_v2) datasets retrieved from the United States Geological Survey (USGS) website were overlaid with the G30cD and used in performing the inundation modeling.

3.2. Tide Gauge Stations

We set eight tide gauges as output points (Figure 3) to obtain the tsunami height and arrival time. Among these stations, only Advanced Science and Technology Institute (ASTI) is an actual tide gauge station. Japan International Cooperation Agency (JICA) is a proposed tide gauge station to be installed in early part of 2014. NAMRIA tide gauge is a pre-existing tide level monitoring station maintained by NAMRIA. The other 5 tide gauge stations are assumed in this study.

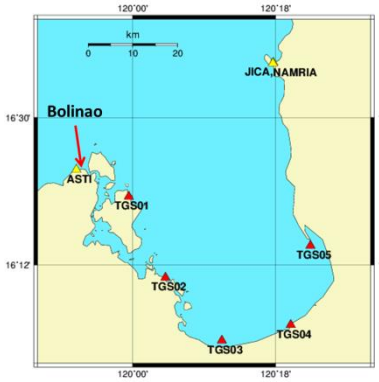

Figure 3. Location of the tide gauge stations set as output points.

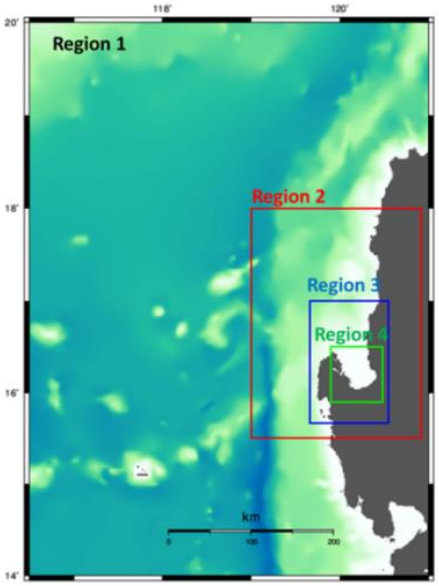

Figure 4. Computation regions for tsunami height and arrival time (region 1) and tsunami inundation (regions 1 to 4).

3.3. Tsunami Simulation

To model the tsunami propagation, we used the tsunami simulation codes; Tohoku University Numerical Analysis Model for Investigation of Near-field Tsunamis, No. 2 (TUNAMI-N2) by Imamura et al. (2006). In this study, we used the tsunami simulation codes provided by Koshimura (2013), which were modified by Fujii (2013) for the NetCDF input and output. We also used the simulation codes for tsunami inundation by Yanagisawa (2013). The tsunami height calculations using the uniform grid system of 1' in Cartesian coordinates were set in region 1 (Figure 4). The tsunami inundation calculations using the Spherical coordinates were set in four regions as seen in Figure 4. The spatial grid sizes of regions 1 to 4 are 1', 20", 6.66667", and 2.22222", respectively.

3.4. Earthquake Source

In this study, we used the fault parameters of the segment 2 of Manila Trench (MT2) as shown in Table 1. We simulated two earthquake case scenarios of the historical (Case 1) and

maximum credible (Case 2) tsunamis. For the case scenarios, we considered the biggest historical event (M7.6) that ever occurred within this segment and the maximum credible event (M8.4) that can happen along this fault segment (Salcedo, 2010).

Table 1. Fault parameters for each case scenario earthquake.

Scenario	M	Location (lon., lat. (deg))		Length (km)	Width (km)	strike (deg)	dip (deg)	rake (deg)	Slip (m)	Depth (m)
Historical	7.6	119.10	16.06	97.72	53.21	1	36	95	1.21	0
Max Credible	8.4	119.10	16.06	254.0	91.16	1	36	95	3.69	0

3.5. Numerical Stability

The Courant Friedrics Lewy (CFL) condition is given by the formula $\Delta t \leq \frac{\Delta x}{\sqrt{2gh_{max}}}$ (Imamura et al., 2006), where Δt and Δx are the temporal and spatial length of grids respectively, g is the gravity acceleration (9.8 m/s^2) and h_{max} is the maximum still water depth in a computation region. In this study, we used temporal grid size (Δt) of 3.0 s in simulations of tsunami height and travel time and 1.0 s in inundation calculation to stabilize the numerical computations.

4. RESULTS AND DISCUSSIONS

4.1. Ocean Floor Deformation and Tsunami Propagation

Figure 5 shows the seafloor deformation of the two earthquake scenarios. The Case 1 earthquake scenario had a computed maximum uplift of 0.64 m while the maximum subsidence was 0.26 m. Case 2 had a computed maximum uplift of 1.87 m and the maximum subsidence was 0.31 m.

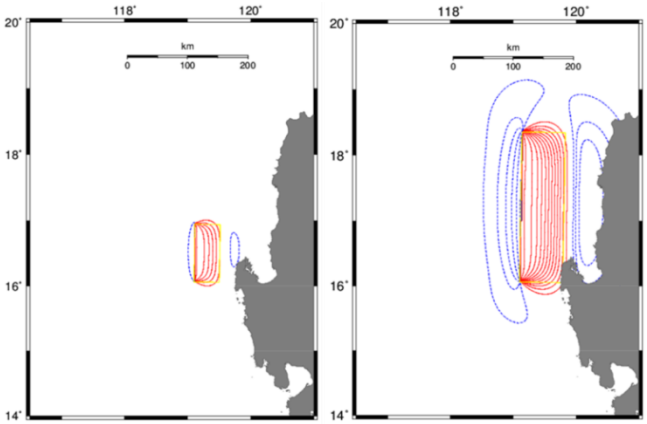

Figure 5. Seafloor deformations for Cases 1 (left) and 2 (right). The contour intervals of uplift (red lines) and subsidence (blue broken lines) are 0.1 m and 0.05 m, respectively.

4.2. Tsunami Waveforms

Figure 6(a) shows the comparison of the tsunami waveforms produced using the G1m and G30c in Case 2. The waveforms calculated at TGS01, TGS02, TGS03, TGS04, and TGS05 have remarkable differences. The tide gauge stations were located in the inner bay of the Lingayen Gulf, while the tide gauge stations that calculated almost the same waveform amplitudes were located outside the Lingayen Gulf.

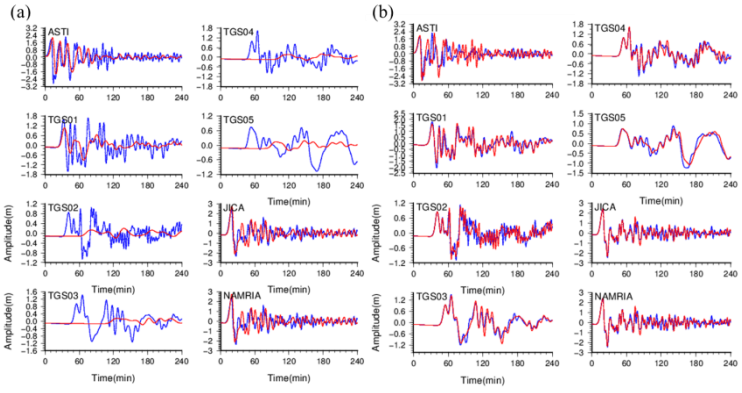

Figure 6. Comparison of tsunami waveforms in Case 2 produced (a) using G1m (red) and G30c (blue) and (b) using G30c (blue) and G30cD (red).

The comparison of the waveforms calculated using the G30c and G30cD in Case 2 are shown in Figure 6(b). The waveforms calculated at all tide gauge stations have almost

the same amplitudes. This shows that the depths of the two bathymetry data are almost identical. This further demonstrates that the use of the two bathymetry data is more realistic than the use of the G1m.

4.3 Tsunami Travel Times (TTT) and Tsunami Heights

Figure 7 shows the estimated TTTs at each tide station for Cases 1 and 2 using the three bathymetry data. The TTTs at tide gauges located in the open sea (ASTI, JICA, and NAMRIA) or near the open sea (TGS01) are almost the same for both the earthquake scenario cases, while the TTTs in the inner bay (TGS02, TGS03, TGS04 and TGS05) using both G30c and G30cD are almost the same. On the other hand, the TTTs at the same tide gauges using G1m are longer. The first tsunami arrives at the Lingayen Gulf (referred also as inner bay) coast in 38 min and 35 min as estimated at TGS02 for the Cases 1 and 2, respectively. Figure 8 shows the tsunami heights at each tide gauge for Cases 1 and 2.The maximum wave height of Case 1 was 0.3 m at TGS03. In Case 2, the maximum tsunami height was 1.6 m at TGS04.

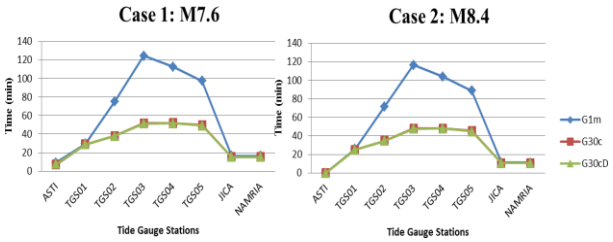

Figure 7. Estimated TTTs from the source point to the tide gauge stations in Cases 1 (left) and 2 (right) using the three different bathymetry data.

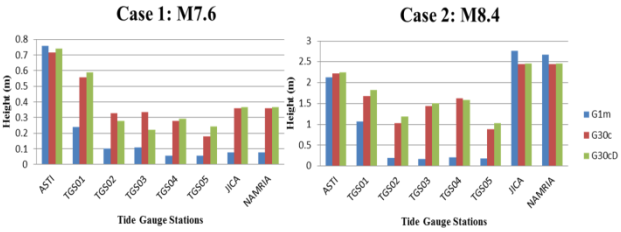

Figure 8. Maximum heights computed at each tide gauge station in Cases 1 (left) and 2 (right) using the three different bathymetry data.

4.4. Tsunami Inundation

We simulated tsunami inundations for Cases 1 and 2 taking their vertical and horizontal effects into consideration. We also simulated Case 2 neglecting the horizontal effect to compare the results with a combination of vertical and horizontal effects. To measure the inundation height, we set three water gauges (WG) as output points in the target area in Dagupan City (Figure 9). The results show that when vertical and horizontal effects are both considered, the highest calculated tsunami height is higher by about 17% as compared to the one calculated neglecting the horizontal effects.

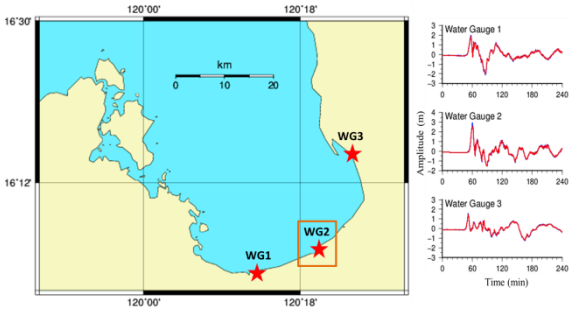

Figure 9. Location of the inundation area analysis (orange box) and water gauges set as output points and the corresponding waveforms at each water gauge (blue; considering the vertical and horizontal effects, red; with vertical effects only).

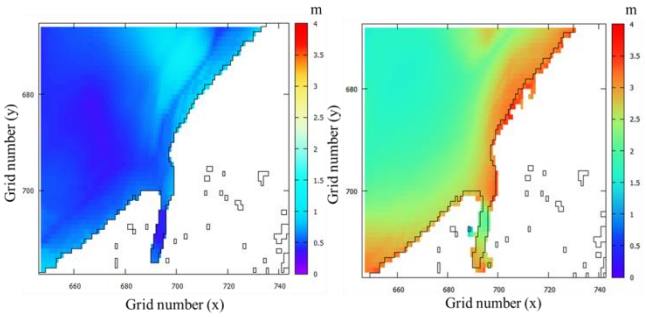

Figure 10. Magnified view of the target area in Dagupan City for inundation analysis of Cases 1 (left) and 2 (right) in WG 2.

The maximum height calculated at WG 2 was 0.7 m in Case 1. The maximum height among the WGs set was 3.0 m at WG 2 in Case 2. The calculated inundation areas in the target area as shown in Figure 10 were approximately 0.13 km^2 and 0.70 km^2 for Cases 1 and 2, respectively.

4.5. Tsunami Sensor

Tsunami sensors can be effective as an early warning system in the inner bay along the Lingayen Gulf coast because the first tsunamis arrive in 38 min and 35 min both recorded at TGS02 for Cases 1 and 2, respectively. Bolinao (see Figure 3) will be hit by tsunamis with a maximum height of 0.8 m (as recorded at ASTI) that will be arrived in 8 min after the earthquake in Case 1. In this case, a quick evacuation is needed to escape the dangers of tsunami. In Case 2, the initial tsunami will attack Bolinao coast in less than 1 min and the wave will reach the positive peak of 2.0 m in 10 min and a maximum height of 2.4 m in about 30 min (as recorded at ASTI). In this case, the aim of the tsunami sensors will be ineffective in the coastal areas of Bolinao. By combining ASTI and JICA tide gauge stations as tsunami sensors, a better and robust early warning system would be achieved as they complemented with each other.

5. CONCLUSIONS

Tsunami simulations were performed for Lingayen Gulf, setting Dagupan City as the target area using the two earthquake scenarios of M8.4 and M7.6 from a segment of the Manila Trench. The use of GEBCO 30 arc-sec data and digitized depth points from a bathymetry map produces a more realistic output as compared to the use of GEBCO 1 arc-min. Also, considering the horizontal displacement effect of tsunami in the simulation is needed to accommodate the influence of the slope of the ocean floor near the trench axis.

ASTI tide gauge station is effective as tsunami warning system in the inner bay of Lingayen Gulf coast while it is ineffective in the Bolinao coast. By combining ASTI and JICA tide gauge stations as tsunami sensors, a more accurate early warning system will be in placed.

The results of the tsunami simulation will give better understanding of the community's tsunami risk that can be used in designing the evacuation strategies and maps.

As part of my future plan, I would like to do tsunami hazard assessments in the populated coastal areas in the Philippines that are prone to tsunamis. The results are essential inputs in the development of tsunami hazard maps. Likewise, I would like to formulate a database of earthquake scenarios that can be useful in establishing a tsunami early warning system in the Philippines.

REFERENCES

Fujii, Y., 2012-2013, Lecture notes on Tsunami simulation, IISEE/BRI.

Imamura F., Yalciner A.C., Ozyurt G., 2006, DCRC, Tohoku University, Japan.

Koshimura S., 2013, TUNAMI-N2 CODE, Tohoku University, 2012-2013 IISEE/BRI Lecture notes.

NAMRIA, 1987, Philippine National Topographic Map Series.

Okada Y., 1985, Surface deformation due to shear and tensile faults in a half space: Bulletin, Seismological Society of America, 75, 1135-1154.

Ramos, N. T., Tsutsumi, H., 2010, Tectonophysics (2010), doi: 10.10 16/j.tecto.2010.08.007.

Salcedo, J., 2010, Individual studies by participant at the IISEE.

Tanioka, Y. and Satake, K., 1996, Tsunami generation by horizontal displacement of ocean bottom, Geophysical Research Letters, Vol. 23, No. 8, 861-864.

Website: NOAA, General bathymetric chart of the oceans (GEBCO) http://ngdc.noaa.gov/mgg/gebco/.

Website: PHIVOLCS official website www.phivolcs.dost.gov.ph.

Website: USGS, http://dds.cr.usgs.gov/srtm/version2_1/SRTM3/Eurasia/.

Yanagisawa, H., 2012-2013, Lecture Notes on Numerical simulation of tsunami and its application, IISEE/BRI.